HHS Public Access

Author manuscript

J Biomech. Author manuscript; available in PMC 2018 November 07.

Published in final edited form as:

J Biomech. 2017 November 07; 64: 258–261. doi:10.1016/j.jbiomech.2017.09.020.

An In Vivo Model of a Mechanically-Induced Bone Marrow Lesion

Jonathan B. Matheny[a,b], **Matthew G. Goff**[a,b], **Sarah L. Pownder**[c], **Matthew F. Koff**[c], **Kei Hayashi**[d], **Xu Yang**[c], **Mathias P. G. Bostrom**[c], **Marjolein C. H. van der Meulen**[a,b,c], and **Christopher J. Hernandez**[a,b,c,*]

[a]Sibley School of Mechanical and Aerospace Engineering, Cornell University, Ithaca, New York, USA

[b]Meinig School of Biomedical Engineering, Cornell University, Ithaca, New York, USA

[c]Hospital for Special Surgery, New York, New York, USA

[d]Department of Clinical Sciences, Cornell University College of Veterinary Medicine, Ithaca, New York, USA

Abstract

Bone marrow lesions (BMLs) are radiologic abnormalities in magnetic resonance images of subchondral bone that are correlated with osteoarthritis. Little is known about the physiologic processes within a BML, although BMLs are associated with mechanical stress, bone tissue microdamage and increased bone remodeling. Here we establish a rabbit model to study the pathophysiology of BMLs. We hypothesized that *in vivo* loads that generate microdamage in cancellous bone would also create BMLs and increase bone remodeling. *In vivo* cyclic loading (0.2 to 2.0 MPa in compression for 10,000 cycles at 2 Hz) was applied to epiphyseal cancellous bone in the distal femurs of New Zealand white rabbits (n=3, right limb loaded, left limb controls experienced surgery but no loading). Magnetic resonance images were collected using short tau inversion recovery (STIR) and T1 weighted sequences at 1 and 2 weeks after surgery/loading and histological analysis of the BML was performed after euthanasia to examine tissue microdamage and remodeling. Loaded limbs displayed BMLs while control limbs showed only a small BML-like signal caused by surgery. Histological analysis of the BML at 2 weeks after loading showed increased tissue microdamage (p=0.03) and bone resorption (p=0.01) as compared to controls. The model described here displays the hallmarks of load-induced BMLs, supporting the use of the model to examine changes in bone during the development, progression and treatment of BMLs.

[*]Corresponding Author: Christopher J. Hernandez, Ph.D., 355 Upson Hall, Cornell University, Ithaca, NY 14853 Phone: (607) 255-5129, Fax: (607) 255-1222, cjh275@cornell.edu.

Conflict of Interest Statement

Dr. van der Meulen has stock ownership in Johnson & Johnson, Novartis, and Proctor & Gamble. Dr. Bostrom is a consultant for Smith and Nephew.

Keywords

Bone Marrow Edema Pattern; Bone Remodeling; Bone Mechanics; Microscopic Tissue Damage; Magnetic Resonance Imaging; Animal Model

Introduction

Bone marrow lesions (BMLs, sometimes referred to as “bone bruises” or “bone marrow edema patterns”) are observed in magnetic resonance images (MRI) of subchondral cancellous bone and occur in chronic and acute joint disorders. BMLs are associated with increased joint pain and joint degeneration, suggesting that physiological processes in bone may influence the health of the entire joint (Tanamas et al., 2010; Xu et al., 2012). The etiology and pathophysiology of BMLs are poorly understood, but appear to be associated with high mechanical stresses in cancellous bone (Eriksen and Ringe, 2012). Biopsies of BMLs show microscopic tissue damage in bone (Taljanovic et al., 2008) as well as increased bone remodeling (Zanetti et al., 2000), woven bone formation, and increased angiogenesis (Shabestari et al., 2016). However, a limitation of biopsies is that they are acquired at the time of total joint replacement and therefore provide little information about the sequence of events in the early, reversible stages of BMLs. Given the challenges in characterizing the pathophysiology of early stage BMLs in patients, a pre-clinical model that recapitulates the pathogenesis of a BML would be valuable for understanding the changes in bone physiology within a BML.

Here we establish an animal model of mechanically-induced BMLs focusing on two specific hypotheses. First, we hypothesized that the loads required to generate microdamage in subchondral cancellous bone would also create BMLs. Second, we hypothesized that regions of cancellous bone with load-induced BMLs would display increased bone remodeling. Following *in vivo* loading, the initiation and progression of BMLs was evaluated using MRI, and the amount of microdamage and bone resorption within the BML was determined.

Methods

Surgical Approach

Given the association between mechanical loading and BMLs, we adapted an *in vivo* loading model in the rabbit to generate a BML. The rabbit loading model has been used extensively to study functional adaptation and implant integration in cancellous bone (Fahlgren et al., 2013; van der Meulen et al., 2006). *In vivo* loading is applied using a loading device implanted by a board certified veterinary surgeon (KH). A 17 mm x 9 mm region of the cortex located distal to the lateral femoral growth plate is ground flat using spherical cutting burrs. A polyether ether ketone (PEEK) implant is placed on the flattened region of the lateral epiphyseal cortex. The implant is secured to the femur using a 2 mm diameter PEEK screw and a 1.5 mm diameter titanium screw. The use of PEEK implants avoids metallic susceptibility artifact during MRI. Following placement of the implant, the cortex (1 mm thickness) beneath the implant is removed using a custom routing device (diameter 4.75 mm). The removal of the cortex made it possible to reliably generate microdamage in

cancellous bone; our previous work has shown that generating microdamage in cancellous bone with intact cortical bone is difficult to achieve over reasonable periods of anesthesia time (Kummari et al., 2009). An aluminum loading platen aligned with the implant is placed through the hole in the cortex and cyclic loading is applied directly to the underlying cancellous bone using a servo-electric loading device (Testbench, Bose-Electroforce, Eden Prairie, MN).

In Vivo Loading and Visualization of BMLs

Animal experiments were performed following approval by the Cornell University Institutional Animal Care and Use Committee in an AAALAC-accredited facility. Male, New Zealand white rabbits (n=3, 7.5 months old, 3.56±0.42 kg, Covance Inc., Princeton, NJ) were housed individually in stainless steel cages in a room with a 12:12 hour light: dark cycle and temperature between 18.9 to 21.1 °C. Rabbits were fed Teklad 15% rabbit diet 8630 (Envigo, Madison, WI) and water *ad libitum* and provided environmental enrichment. Following 2 weeks of acclimation, animal were anesthetized with isoflurane and the implants were placed bilaterally using a posterior lateral surgical approach. The right limbs received implants and were loaded in cyclic compression between 0.2 MPa (minimum) and 2.0 MPa (maximum) at 2 Hz frequency for 10,000 cycles. The loading regimen was determined through pilot studies with identical surgical placement and point of loading as the *in vivo* studies and was found to generate microscopic tissue damage (microdamage) in cancellous bone without causing overt fracture. Prior to closing the surgical site, a PEEK cap was secured within the implant to occupy the hole in the cortex. After surgical closure, the left limb received cortical defect and implant, but no loading was applied. Wounds were washed with antiseptic, and an antibiotic prophylaxis was applied the day of surgery (25 mg/kg ampicillin). Rabbits received buprenorphine (0.05 mg/kg) analgesic for 2 days after surgery and were monitored daily by animal care staff. The surgery/loading was well-tolerated by the rabbits, and no differences in gait between limbs were observed.

At one and two weeks after surgery/loading, animals were anesthetized, and both limbs were evaluated using a clinical 3T MRI scanner (DVMR 750, GE Healthcare, Milwaukee WI) with an 8 channel phased-array transmit/receive (T/R) knee coil (Invivo, Gainesville, FL). T1-weighted and fat-suppressed short tau inversion recovery (STIR) images were collected to visualize BMLs. BML signal was identified and manually segmented by a board certified veterinary radiologist (SLP) using a combination of the STIR and T1 weighted images. BML volume (in mm^3) was calculated as the area of the BML signal within individual slices multiplied by slice thickness (Xu et al., 2012). Animals were euthanized via an intravenous injection of pentobarbital sodium (86 mg/kg) immediately following acquisition of the second MRI dataset.

Following euthanasia, the limbs were dissected free from soft tissue, implants were removed, and microcomputed tomography images of each femur were collected at an isotropic voxel size of 50 μm (eXplore CT-120, GE Healthcare, Milwaukee WI). The lateral epiphysis of each femur was dissected using a low speed precision saw (Buehler, Lake Bluff, Illinois USA), and bone marrow was removed using a low-pressure water jet. To identify microdamage, specimens were bulk stained in calcein solution (0.5 mM) for two hours

under vacuum. Specimens were then embedded undecalcified in polymethyl- methacrylate, and sections from the coronal plane were collected and polished to 100 μm thickness. Images of the sections were obtained using a confocal microscope (Zeiss LSM 710 Confocal Carl Zeiss, Inc., Thornwood, NY USA) to obtain a mosaic of images (4.08 x 4.08 mm with 2.4 μm thickness) and a pixel size of 0.66 μm. A rectangular region of interest (width 3.0 mm, height 3.7 mm) located 500 microns away from contact with the loading platen was selected for analysis. Damage volume fraction (DV/BV, %), and eroded surface (ES/BS, %, identified as scalloped or crenated surfaces), were measured using point counting (21 μm grid spacing). All analyses were conducted using automated approaches or by observers blinded to specimen loading history.

Statistical Analysis

Differences in damage volume fraction and eroded surface between loaded and unloaded groups were identified using two-tailed, paired t-tests (JMP Pro 10.0.2, SAS Institute Inc., Cary, NC, USA). Differences in BML volume between loaded and unloaded groups was determined using repeated measures ANCOVA implemented with a generalized least squares model using time and limb (loaded, non-loaded) as fixed effects and animal as a random effect.

Results

Cyclic loading resulted in the generation of large BML signal visible in both STIR and T1 weighted MR sequences at both one and two weeks after surgery/applied loading (Week 2 images shown in Figure 1B). Small BML-like signal was present in control limbs. Compared to the BML-like signal in control limbs, BMLs in loaded limbs were 174% larger in volume at week 1 and 228% larger at week 2 and extended farther from the surface ($p=0.01$, Figures 1B and 1E).

Bone tissue collected from BMLs displayed tissue microdamage and evidence of increased bone resorption at two weeks after surgery/loading (Figure 4A–C). Loaded limbs had 411% more stained microdamage (damage volume fraction: Loaded 3.68±0.30 (2.94, 4.41) % vs. Control 0.7±0.7 (−0.97, 2.41) %, mean±SD, (95% CI), $p=0.03$, Figure 1D) and 177% greater eroded surface compared to contralateral control limbs (Loaded 17.20±2.72 (10.44, 23.96) % vs. Control 6.21±1.95 (1.37, 11.05) %, $p=0.01$, see Figure 1F). Damage volume fraction was correlated with BML volume ($R^2=0.85$, $p=0.009$, see Figure 1G).

Discussion

The goal of the current study was to establish a preclinical model of a bone marrow lesion. We showed that *in vivo* mechanical loading in epiphyseal cancellous bone could result in a BML visible at 1 and 2 weeks following loading. Tissue microdamage and increased bone resorption (as measured by eroded surface) were present within regions of bone tissue within the bone marrow lesion. These features recapitulate the hallmarks of load-induced BMLs observed in clinical biopsies.

Our findings are consistent with current hypotheses that microdamage created by mechanical loading leads to increased bone remodeling and BMLs. Tissue microdamage has long been considered a stimulus for bone resorption and remodeling. In cortical bone, the generation of tissue microdamage causes apoptosis of osteocytes in the immediate vicinity of microdamage which leads to increased RANKL expression in osteocytes surrounding the microdamage followed by subsequent increases in bone resorption and remodeling (Kennedy et al., 2014; Kennedy and Schaffler, 2012). In cancellous bone, the response to tissue microdamage is unknown. The presence of tissue microdamage and increased bone resorption in BMLs in the current study, however, is consistent with prior work in cortical bone suggesting that the mechanism in cancellous bone may be similar. However, tissue damage in cancellous bone has also been associated with increased bone formation in the form of a “microcallus”(Hahn et al., 1995) and examination of additional time points would be required to determine the role of increased bone formation following the appearance of tissue microdamage. In addition, our findings are consistent with studies of subchondral cancellous bone in mice which showed that increases in mechanical loading caused by ACL transection leads to increased subchondral bone resorption, and development of a small BML before the leading to cartilage degeneration (Zhen et al., 2013).

The pre-clinical model described here has a number of strengths as a tool for studying BMLs. First, the model includes two characteristics that are observed in biopsies of established BMLs in humans: tissue microdamage and evidence of increased bone remodeling (measured as increased eroded surface). Second, the model uses skeletally mature rabbits. Skeletally mature animals have closed growth plates which ensures that changes in cancellous bone microarchitecture are due to the applied mechanical stimulus and not longitudinal growth(Turner, 2001). A final strength is that the BMLs in the model were created by applying loads directly to epiphyseal cancellous bone, allowing examination of the BMLs without direct damage to cartilage or ligaments. In future studies, the interaction and synergy between cartilage damage and BMLs can be explored by directly damaging cartilage with and without underlying BMLs (Gregory et al., 2012). Furthermore, by loading only bone, the effect of bone physiology can be isolated from the rest of the joint, and by applying the load off axis we are able to generate microdamage at lower applied strain levels because the bone is not adapted to loading in this direction. As a result, the loading model also created microdamage without causing overt fracture to the epiphysis, and no evidence of a fracture healing response was observed.

A limitation of the current study is the small sample size (n=3 paired limbs). Although the number of limbs examined was small, the differences between loaded and control limbs were large, consistent among all three animals, and differences between loaded and control limbs were apparent ($p<0.03$), providing confidence in the repeatability of the model. Small BML-like signal was observed in control limbs; however, the signal appeared closer to the surface than the load-induced BMLs and was likely associated with the surgery induced damage on the surface. We examined histology at a single time point; therefore, our results provide only rudimentary information regarding the longitudinal changes of the bone. Little is known about the etiology of BMLs, and it is unclear how well the pathophysiology of a load-induced BML resembles that of BMLs associated with other clinical conditions.

Clinical evidence indicates that changes in bone physiology precede the development of osteoarthritis and may even be a potential target for preventive treatment. By representing the major components of a clinical BML, this *in vivo* rabbit model has the potential to provide important information on the natural history and efficacy of treatments on load-induced BMLs.

Acknowledgments

This work was supported by funding from the National Institute of Arthritis and Musculoskeletal and Skin Diseases of the National Institute of Health under awards AR57362 and AR00728. One of the authors (JBM) received funding from the NSF Graduate Research Fellowship Program. We thank Bhupinder Singh and the Cornell CARE facility for their assistance in animal care and housing and surgery. We thank Teresa Porri and the Cornell MRI facility for their assistance in microcomputed tomography and MR imaging. We also thank Hollis Potter for her advice.

References

Eriksen EF, Ringe JD. Bone marrow lesions: a universal bone response to injury? Rheumatol Int. 2012; 32:575–584. [PubMed: 21901347]

Fahlgren A, Yang X, Ciani C, Ryan JA, Kelly N, Ko FC, van der Meulen MCH, Bostrom MPG. The effects of PTH, loading and surgical insult on cancellous bone at the bone-implant interface in the rabbit. Bone. 2013; 52:718–724. [PubMed: 22613252]

Gregory MH, Capito N, Kuroki K, Stoker AM, Cook JL, Sherman SL. A review of translational animal models for knee osteoarthritis. Arthritis. 2012; 2012:764621. [PubMed: 23326663]

Hahn M, Vogel M, Amling M, Ritzel H, Delling G. Microcallus formations of the cancellous bone: a quantitative analysis of the human spine. J Bone Miner Res. 1995; 10:1410–1416. [PubMed: 7502714]

Kennedy OD, Laudier DM, Majeska RJ, Sun HB, Schaffler MB. Osteocyte apoptosis is required for production of osteoclastogenic signals following bone fatigue in vivo. Bone. 2014; 64:132–137. [PubMed: 24709687]

Kennedy OD, Schaffler MB. The roles of osteocyte signaling in bone. The Journal of the American Academy of Orthopaedic Surgeons. 2012; 20:670–671. [PubMed: 23027697]

Kummari SR, Davis AJ, Vega LA, Ahn N, Cassinelli EH, Hernandez CJ. Trabecular microfracture precedes cortical shell failure in rat caudal vertebrae under cyclic loading. Calcif Tiss Int. 2009; 85:127–133.

Shabestari M, Vik J, Reseland JE, Eriksen EF. Bone marrow lesions in hip osteoarthritis are characterized by increased bone turnover and enhanced angiogenesis. Osteoarthritis Cartilage. 2016; 24:1745–1752. [PubMed: 27233775]

Taljanovic MS, Graham AR, Benjamin JB, Gmitro AF, Krupinski EA, Schwartz SA, Hunter TB, Resnick DL. Bone marrow edema pattern in advanced hip osteoarthritis: quantitative assessment with magnetic resonance imaging and correlation with clinical examination, radiographic findings, and histopathology. Skeletal Radiol. 2008; 37:423–431. [PubMed: 18274742]

Tanamas SK, Wluka AE, Pelletier JP, Pelletier JM, Abram F, Berry PA, Wang YY, Jones G, Cicuttini FM. Bone marrow lesions in people with knee osteoarthritis predict progression of disease and joint replacement: a longitudinal study. Rheumatology. 2010; 49:2413–2419. [PubMed: 20823092]

Turner AS. Animal models of osteoporosis--necessity and limitations. Eur Cell Mater. 2001; 1:66–81. [PubMed: 14562261]

van der Meulen MC, Morgan TG, Yang X, Baldini TH, Myers ER, Wright TM, Bostrom MP. Cancellous bone adaptation to in vivo loading in a rabbit model. Bone. 2006; 38:871–877. [PubMed: 16431171]

Xu L, Hayashi D, Roemer FW, Felson DT, Guermazi A. Magnetic resonance imaging of subchondral bone marrow lesions in association with osteoarthritis. Semin Arthritis Rheum. 2012; 42:105–118. [PubMed: 22542276]

Zanetti M, Bruder E, Romero J, Hodler J. Bone marrow edema pattern in osteoarthritic knees: Correlation between MR imaging and histologic findings. Radiology. 2000; 215:835–840. [PubMed: 10831707]

Zhen GH, Wen CY, Jia XF, Li Y, Crane JL, Mears SC, Askin FB, Frassica FJ, Chang WZ, Yao J, Carrino JA, Cosgarea A, Artemov D, Chen QM, Zhao ZH, Zhou XD, Riley L, Sponseller P, Wan M, Lu WW, Cao X. Inhibition of TGF-beta signaling in mesenchymal stem cells of subchondral bone attenuates osteoarthritis. Nat Med. 2013; 19:704–712. [PubMed: 23685840]

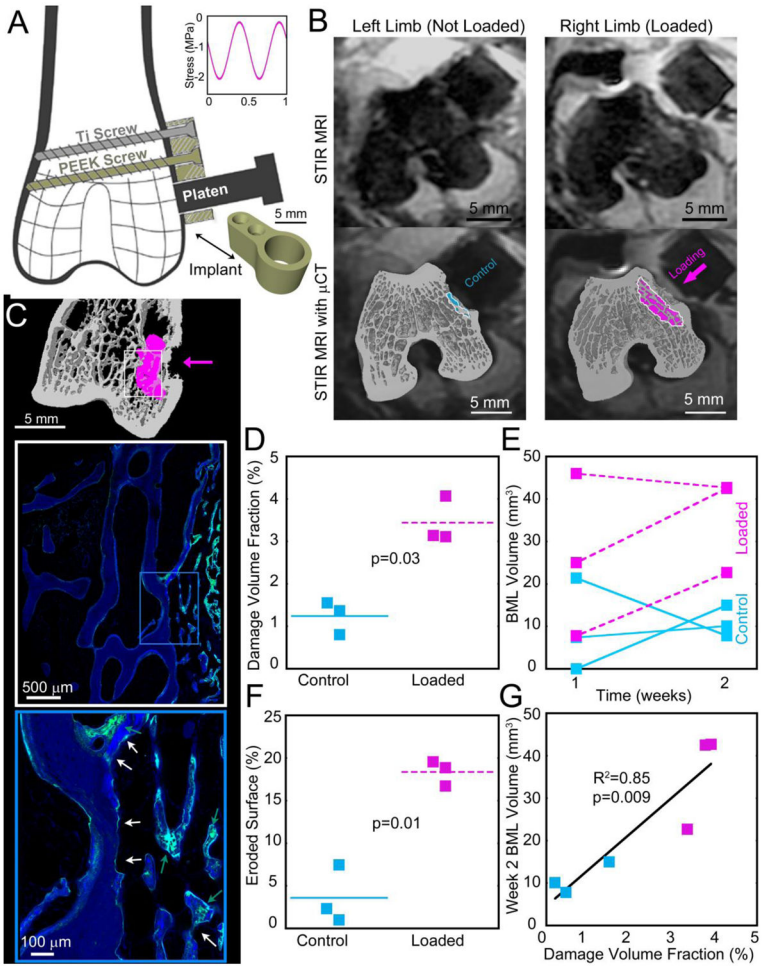

Fig. 1.

(A) The rabbit *in vivo* loading device is shown. A PEEK implant (gold) is surgically fixed to the lateral epiphysis of the femur by Titanium and PEEK bicortical screws. Cyclic compressive loading is applied directly to the underlying cancellous bone. (B) *In vivo* cyclic loading induced the formation of bone marrow lesions (BMLs) evident 1 and 2 weeks after loading. STIR MR images for loaded and control limbs acquired 2 weeks after surgery/loading are shown in the upper frames. The lower frames display microCT images overlaid on STIR MR images with the BML in loaded limbs (light pink) and BML-like signal in control limb (light blue) labeled. (C) A microCT image of a loaded limb with an overlay of the MR image of the BML 2 weeks after loading illustrates the region of interest for histology. The magnified section in the blue box shows microdamage (stained with calcein, green arrows) and eroded surfaces (white arrows) that were evident in the loaded limbs. (D–F) Damage volume fraction, BML volume and eroded surface were greater in loaded limbs. Lines in E connect measurements from the same limb. (G) Damage volume fraction was correlated with BML volume at two weeks after loading.